

**Supplementary Material for
« Shape and composition effects on the Debye temperature
and breathing frequency of metal nanoparticles »**

W. Rigaut^{1,2} and F. Calvo¹

¹Université Grenoble Alpes, CNRS, LiPhy, 38000 Grenoble, France

²Institut Néel, CNRS, Université Grenoble Alpes, F38042 Grenoble Cedex, France

Table of contents

1. Breathing frequencies obtained from various approximations for small nanoparticles
2. Main geometrical features of gold nanoparticles with rounded shapes
3. Main geometrical features of iron nanoparticles with rounded shapes
4. Main geometrical features of elongated and flattened gold nanoparticles
5. Main geometrical features of elongated and flattened iron nanoparticles
6. Surface fractions for pure nanoparticles
7. Main geometrical features of multilayer icosahedral gold and silver nanoparticles
8. Fraction of heterobonds in multilayer icosahedral gold and silver nanoparticles

1. Breathing frequencies obtained from various approximations for small nanoparticles

The accuracy of the uniform harmonic motion for the radial breathing mode was assessed against fully harmonic calculations, in which the fundamental radial breathing mode is identified as the specific harmonic mode that maximises the radial projection of its eigenvector. The specific cases of the icosahedral and cuboctahedral Au_{147} , as well as the truncated octahedral Fe_{1013} , are illustrated in Fig. S1, in which the discrete harmonic spectra are shown with the magnitude of the radial projection as their intensity, in comparison with the continuous power spectra obtained from MD simulations at 300 K for the same systems.

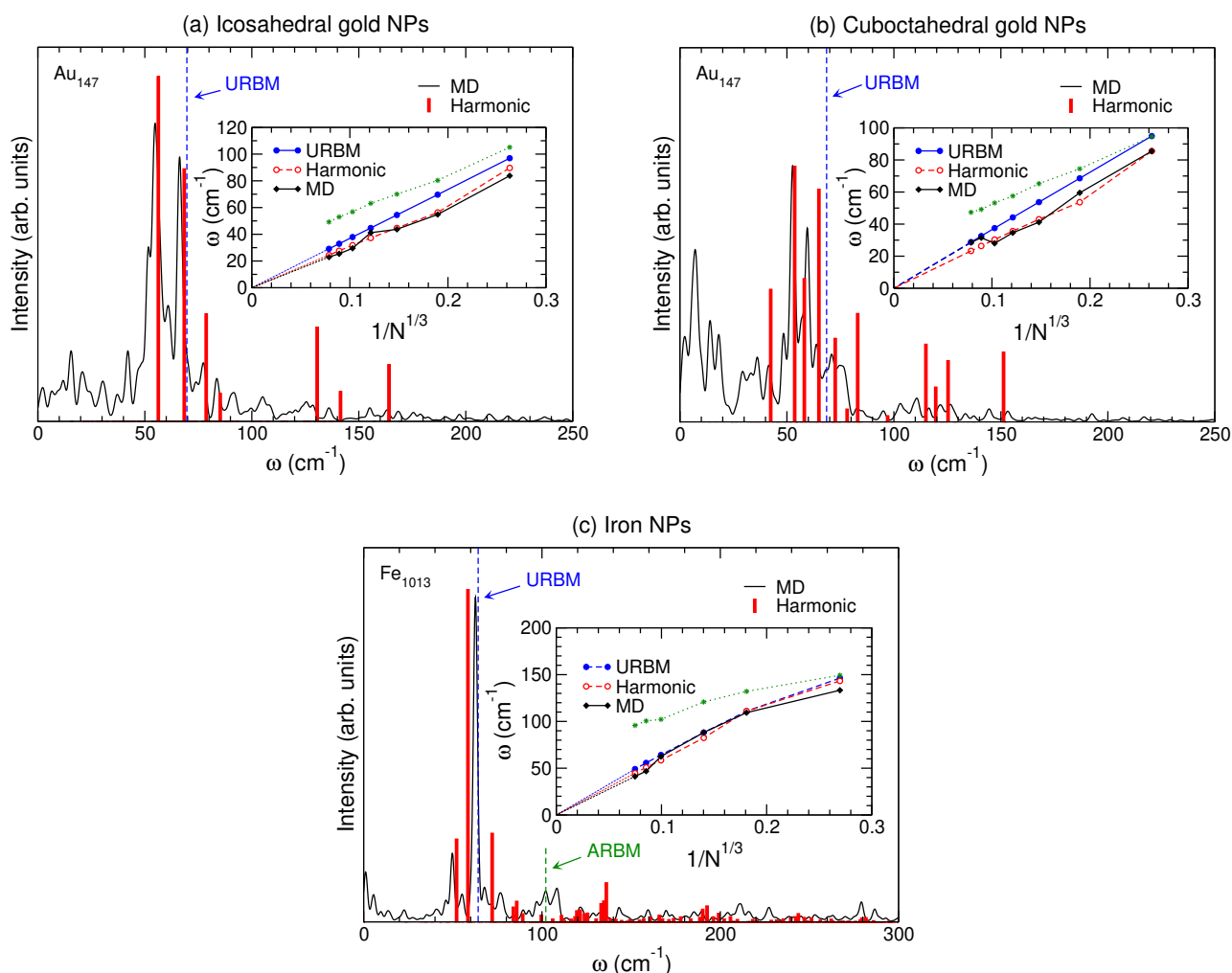


Figure S1. Comparison of the radial breathing frequency obtained from various methods for selected (a) icosahedral gold nanoparticles; (b) cuboctahedral gold nanoparticles; (c) iron nanoparticles of truncated octahedral (Wulff) shape. The main figures show the power spectra of the volume for selected nanoparticles (black solid lines), the magnitude of the radial projections of the harmonic eigenvectors (red bars), and the prediction of the uniform radial breathing mode (URBM, vertical blue dashed line). The insets represent the corresponding variations of the radial breathing frequency for nanoparticles with varying size, as a function of $N^{-1/3}$, and the green stars indicate the radial breathing frequency obtained by averaging the harmonic values according to their relative radial component. The specific value obtained from this averaging method is highlighted in panel (c) for the the iron nanoparticle and denoted as ARBM.

Overall, the power spectra share the same features as the discrete harmonic spectra, and in particular they may exhibit competing peaks that indicate several contribution to the breathing motion. Anharmonicities generally result in a small but appreciable redshift. Noteworthy, the prediction from the uniform radial harmonic approximation falls very close to an existing peak in the entire harmonic spectrum, even though it may not be the most intense from the point of view of its projection magnitude but only second (Au_{147}). This consequently leads to an overestimation of the radial breathing frequency for these gold particles.

Owing to their lower symmetry, cuboctahedral particles exhibit even more modes that are radially active according to the weight, given by the magnitude of P_k [see Eq. (8) of main article]. Assignment of the radial breathing frequency is consequently even more difficult, as illustrated in Fig. S1(b) for the 147-atom particle.

Extending these results to a broader size range, the variations of the radial breathing mode against inverse nanoparticle radius, shown as insets in Fig. S1, confirm these trends, and indicates that the uniform radial harmonic approximation is almost quantitative for Wulff-shaped iron nanoparticles, although it systematically overshoots in the case of icosahedral gold particles owing to the competing modes.

For these nanoparticles an average radial breathing mode was determined, still in the harmonic approximation, by averaging the entire set of harmonic frequencies using $|P_k|$ as a weight. As shown in the insets of Fig. S1, the resulting values significantly overestimate both the uniform radial breathing mode [Eq. (9) of main article] and the maximum of the anharmonic power spectra extracted from MD simulations, except in the smallest clusters. The discrepancy even exceeds 40 % for the larger particles such as Fe₁₀₁₃ [see Fig. S1(c)].

2. Main geometrical features of gold nanoparticles with rounded shapes

Table S1. Maximum outer radius and number of atoms in gold nanoparticles with rounded shapes, as a function of the rounding exponent m

Rounding exponent m	Outer maximum radius (Å)	Number of atoms
0.5	122.0	10443
0.75	67.0	10438
1	47.0	10170
1.25	41.0	10130
1.5	38.0	10791
1.75	35.0	10462
2	33.0	10149
2.25	32.0	10288
2.5	31.0	10187
3	30.0	10451
3.5	29.0	10067
4	29.0	10475
5	28.0	10355
6	27.6	10427
7	27.37	10307
8	27.32	10339
9	27.32	10483
10	27.31	10495

3. Main geometrical features of iron nanoparticles with rounded shapes

Table S2. Maximum outer radius and number of atoms in iron nanoparticles with rounded shapes, as a function of the rounding exponent m

Rounding exponent m	Outer maximum radius (Å)	Number of atoms
0.75	59.0	10009
1	45.0	10431
1.25	37.8	10035
1.5	34.2	10103
1.75	31.5	10175
2	30.5	10177
2.25	29.3	10081
2.5	28.5	10027
3	27.5	10299
3.5	26.7	10107
4	26.2	10131
5	25.8	10307
6	25.5	9965
7	25.4	10129
8	25.2	10153
9	24.7	10105
10	24.45	9925

4. Main geometrical features of elongated and flattened gold nanoparticles

Table S3. Maximum outer dimensions along the x, y, and z dimensions and number of atoms in deformed gold nanoparticles, as a function of the prolateness parameter P

Prolateness	Dimensions along X and Y axes (Å)	Dimension along Z axis (Å)	Number of atoms
-0.198	29.0	6.0	10463
-0.197	28.3	6.5	10159
-0.180	27.5	7.0	10521
-0.179	27.0	7.5	10309
-0.177	26.5	8.0	10413
-0.176	26.2	8.5	10237
-0.155	25.0	9.0	10381
-0.154	24.3	9.5	10381
-0.152	24.5	10.0	10421
-0.150	24.3	10.5	10285
-0.128	24.0	11.0	10479
-0.125	13.3	11.5	10491
-0.123	23.0	12.0	10411
-0.105	22.3	12.5	10475
-0.093	22.3	13.0	10231
-0.090	22.0	13.5	10399
-0.089	21.4	14.0	10239
-0.071	20.8	14.5	10477
-0.061	20.4	15.0	10381
-0.059	20.3	15.5	10357
-0.057	20.3	16.0	10453
-0.032	20.0	16.5	10373
-0.027	19.5	17.0	10341
0	18.5	18.5	10410
0.042	17.5	20.5	10204
0.053	17.0	22.0	10308
0.081	16.5	23.0	10396
0.119	16.0	25.0	10226
0.142	15.5	26.5	10498
0.147	15.0	27.5	10410
0.175	14.5	29.0	10436
0.219	14.0	32.0	10422
0.232	13.5	33.5	10454
0.243	13.0	34.0	10398
0.275	12.5	36.5	10360
0.307	12.0	40.5	10425
0.316	11.5	44.5	10365
0.329	11.0	43.0	10359
0.381	10.5	51.0	10415
0.390	10.0	53.0	10479
0.395	9.5	54.2	10477
0.406	9.0	57.0	10397
0.436	8.5	67.0	10459
0.441	8.0	69.0	10419
0.445	7.5	71.0	10489
0.454	7.0	76.0	10499
0.470	6.5	89.0	10447
0.473	6.0	93.0	10449

5. Main geometrical features of elongated and flattened iron nanoparticles

Table S4. Maximum outer dimensions along the x, y, and z dimensions and number of atoms in deformed iron nanoparticles, as a function of the prolateness parameter P

Prolateness	Dimensions along X and Y axes (Å)	Dimension along Z axis (Å)	Number of atoms
-0.180	24.0	6.0	10015
-0.178	23.9	6.5	9919
-0.165	23.0	7.0	10119
-0.160	22.5	7.5	9987
-0.159	22.45	8.0	9979
-0.144	21.5	8.5	10073
-0.139	21.2	8.0	10033
-0.138	21.1	9.5	10057
-0.122	20.6	10.0	10105
-0.116	20.0	10.5	10017
-0.104	19.7	11.0	10135
-0.091	19.5	11.5	9963
-0.088	19.2	11.0	10139
-0.074	18.5	12.5	9955
-0.065	18.3	11.0	10163
-0.062	18.15	13.5	10051
-0.043	17.8	14.0	10125
-0.032	17.0	15.0	9957
-0.014	16.8	15.5	10217
-0.011	16.75	16.0	10169
0	16.5	16.5	9941
0.015	16.0	17.0	10063
0.038	15.5	18.2	10031
0.074	15.0	19.8	10129
0.078	14.5	20.5	10001
0.103	14.0	21.5	9997
0.136	13.5	23.5	9947
0.154	13.0	24.5	10091
0.178	12.5	26.0	9949
0.218	12.0	28.5	10095
0.226	11.5	29.5	9991
0.263	11.0	32.0	9933
0.287	10.5	34.0	9971
0.303	10.0	35.8	10107
0.353	9.5	41.5	10047
0.363	9.0	43.0	10057
0.374	8.5	45.2	10041
0.404	8.0	50.5	9997
0.414	7.5	53.0	10039
0.428	7.0	57.0	9995
0.444	6.5	63.0	10007
0.449	6.0	66.0	9945

6. Surface fractions for pure nanoparticles

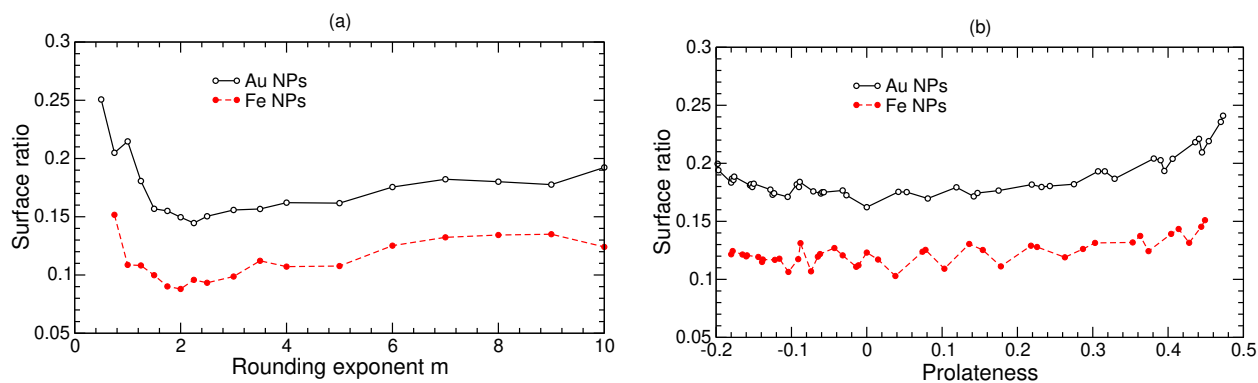


Figure S2. Fraction of surface atoms in gold and iron nanoparticles, as a function of (a) the rounding exponent m ; (b) the prolateness parameter, as determined using a maximum bond criterion of 3 Å.

7. Main geometrical features of icosahedral gold and silver nanoparticles

Table S5. Number of atoms and maximum radial distance for multilayer icosahedral gold and silver nanoparticles, as a function of the number of layers

Numer of layers	Number of atoms	Maximum atomic radius (Au)	Maximum atomic radius (Ag)
2	55	5.36	5.42
3	147	8.11	8.17
4	309	10.86	10.93
5	561	13.62	13.70
6	923	16.38	16.47
7	1415	19.15	19.24
8	2057	21.92	22.02
9	2869	24.70	24.80
10	3871	27.47	27.57
11	5083	30.25	30.35
12	6525	33.03	33.13
13	8217	35.80	35.91
14	10179	38.58	38.69
15	12431	41.36	41.48
16	14993	44.14	44.26

8. Fraction of heterobonds in icosahedral gold and silver nanoparticles

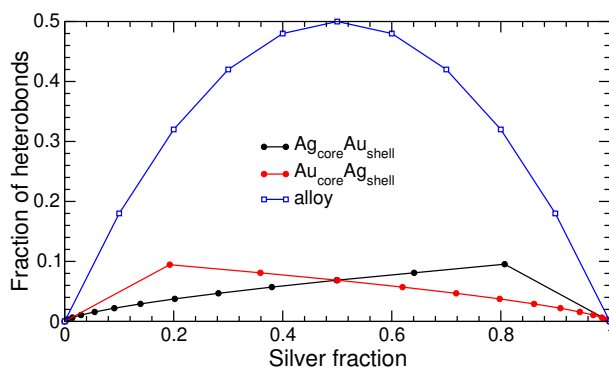


Figure S3. Fraction of Ag-Au bonds in mixed gold and iron nanoparticles, as a function of increasing silver composition, for core-shell and alloyed particles